A Bayesian k-vector Estimation Method for Electromagnetic Waves in Magnetized Cold Plasma

Yuji Tanaka[1], Mamoru Ota[2], Shoya Matsuda[3], and Yoshiya Kasahara[3]

[1] Division of Electrical Engineering, Graduate School of Engineering, Kyoto University, Kyotodaigaku-Katsura, Nishikyo-ku, Kyoto, Kyoto, Japan; e-mail: tanaka.yuji.2m@kyoto-u.ac.jp

[2] Department of Electrical and Control Systems Engineering, National Institute of Technology, Toyama College, 13 Hongo-machi, Toyama, Toyama, Japan; e-mail: m-ota@nc-toyama.ac.jp

[3] Division of Electrical Engineering and Computer Science, Graduate School of Natural Science and Technology, Kanazawa University, Kakuma, Kanazawa, Ishikawa, Japan; e-mail: matsuda@staff.kanazawa-u.ac.jp; kasahara@staff.kanazawa-u.ac.jp

Abstract

Using the plasma wave characteristics and remote sensing technology, the k-vector direction of plasma waves can provide important information for understanding the global features of space plasma. In this study, we proposed a Bayesian k-vector estimation method in magnetized cold plasma based on the wave distribution function method. The proposed method can be applied to various types of sensors with easy visualization and calculation of the estimation accuracy. We verified the effectiveness of the proposed method through simulations.

1. Introduction

The analysis of plasma waves obtained from in-situ observations through scientific satellites is effective for understanding the physics of near-Earth space and space plasmas in general. To measure plasma waves in bands from a few Hz to several tens of kHz, a scientific satellite is generally equipped with orthogonally aligned dipole antennas and a tri-axis search coil (e.g. [1, 2]). The k-vector direction of plasma waves, through the use of plasma wave characteristics and remote sensing technology, provides key information for understanding the global features of space plasma (e.g. [3]).

The k-vector direction is generally estimated using a spectral matrix, which is the correlation matrix of the electromagnetic field. Ideally, determining the k-vector direction including the absolute direction requires the observation results of at least 5 electromagnetic field components. However, estimation of the k-vector direction is often needed when some sensors are ineffective due to sensor damage or some constraints of the scientific satellites. Moreover, the k-vector direction should be estimated with different sensor noise levels. In addition, the extent of estimation accuracy depends on not only the type of sensors but also the averaging number of the spectral matrix. The extent of estimation accuracy should be calculated to realize the detailed propagation analysis.

In this study, we proposed a Bayesian k-vector estimation method in magnetized cold plasma based on the wave distribution function (WDF) method [4, 5]. By introducing the WDF method and the noise integration kernel (NIK) at different sensor noise levels [6], the proposed method can be applied to various types of sensors. In this study, the proposed method adopts the Bayesian inference under the assumption that the number of arriving quasi-plane waves is 1, and it can visualize, and easily calculate the corresponding estimation accuracy.

2. Bayesian k-vector Estimation Method for Electromagnetic Waves in Magnetized Cold Plasma

Our proposed method can be used to visualize the extent of estimation accuracy by calculating the posterior distribution of each k-vector direction under the assumption that the number of arriving quasi-plane waves is 1.

The observation model of the spectral matrix $S(\omega,\theta,\phi)$ can be expressed as:

$$S(\omega,\theta,\phi)=\varepsilon\Sigma+fa(\omega,\theta,\phi)a^{\mathrm{H}}(\omega,\theta,\phi)\ , \qquad (1)$$

where $\varepsilon\geq 0$ is the noise level, the superscript H represents the complex conjugate transpose symbol, Σ is the NIK based on the ratio of sensor noise levels [6], and $f\geq 0$ is the energy of the arriving waves (WDF), and $a(\omega,\theta,\phi)\in\mathbb{C}^D$ (D is the number of sensors) is the amplitude and phase relation (known as the steering vector [7]) at the direction of arrival (θ,ϕ) with a central angular frequency ω. The effect of cold plasma is included in $a(\omega,\theta,\phi)$ which is uniquely determined from a priori information such as plasma density and background magnetic field intensity.

The proposed method considers the probabilistic model for parameters θ,ϕ,f, and ε and the estimated value of the spectral matrix $\hat{R}$ using the observation signals.The joint probability distribution $p(\hat{R},\varepsilon,f,\theta,\phi)$ can be expressed as:

$$p(\hat{R},\varepsilon,f,\theta,\phi)= \qquad (2)$$

$$p(\hat{R}\mid\varepsilon,f,\theta,\phi)p(\varepsilon\mid\theta,\phi)p(f\mid\theta,\phi)p(\theta)p(\phi),$$

where $p(\hat{R}\mid\varepsilon,f,\theta,\phi)$ $p(\varepsilon\mid\theta,\phi)$, $p(f\mid\theta,\phi)$ $p(\theta)$ and $p(\phi)$ show the likelihood distribution of $\hat{R}$ and the prior distributions of ε , f , θ and ϕ respectively.

From N independent observations $x(\nu\Delta T)\in\mathbb{C}^D$ $(\nu=1,\ldots,N)$ ΔT the sampling period), $\hat{R}$ can be expressed using sample matrix inversion [7] as:

$$\hat{R}=\frac{1}{N}\sum_{\nu=1}^{N}x(\nu\Delta T)x^{\mathrm{H}}(\nu\Delta T). \qquad (3)$$

We set the likelihood distribution of $\hat{R}$ to follow a D-dimensional complex Wishart distribution, with $N(\geq D)$ degrees of freedom as given by:

$$p(\hat{R}\mid\varepsilon,f,\theta,\phi)\propto\frac{\left[\det(\Sigma)\right]^N}{\left[\det(\hat{R})\right]^{N-D}}\cdot$$

$$\frac{\exp\left[-N\cdot\mathrm{tr}\left(\left(\varepsilon\Sigma+fa(\omega,\theta,\phi)a^{\mathrm{H}}(\omega,\theta,\phi)\right)^{-1}\hat{R}\right)\right]}{\varepsilon^{ND}\left[\det\left(I_D+\frac{f}{\varepsilon}\Sigma^{-1}a(\omega,\theta,\phi)a^{\mathrm{H}}(\omega,\theta,\phi)\right)\right]^N}\ , \qquad (4)$$

where $\det(\cdot)$ is the determinant and $\mathrm{tr}(\cdot)$ is the sum of diagonal components (trace) [8, 9].

Our proposed method assumes that $p(\varepsilon\mid\theta,\phi)$ $p(f\mid\theta,\phi)$ $p(\theta)$ and $p(\phi)$ are noninformative priors, and the posterior distribution $p(\theta,\phi\mid\hat{R})$ can be expressed as:

$$p(\theta,\phi\mid\hat{R})\propto\int_0^\infty\int_0^\infty p(\hat{R}\mid\varepsilon,f,\theta,\phi)\,\mathrm{d}f\,\mathrm{d}\varepsilon$$

$$\propto\frac{1}{\eta(\theta,\phi)\,p_{\mathrm{beta}}(r_N(\theta,\phi)\mid N,L_N+1)}\cdot$$

$$\left[1-L_N\sum_{\ell=0}^{N-2}\frac{p_{\mathrm{beta}}(r_N(\theta,\phi)\mid\ell+1,L_N+1)}{(L_N+\ell)(L_N+\ell+1)}\right], \qquad (5)$$

where $\Gamma(\cdot)$ is the Gamma function and

$$\eta(\theta,\phi)=a^{\mathrm{H}}(\omega,\theta,\phi)\Sigma^{-1}a(\omega,\theta,\phi)\ , \qquad (6)$$

$$p_{\mathrm{beta}}(r_N(\theta,\phi)\mid\alpha,\beta)=\frac{\Gamma(\alpha+\beta)}{\Gamma(\alpha)\Gamma(\beta)}r^{\alpha-1}(1-r)^{\beta-1}, \qquad (7)$$

$$r_N(\theta,\phi)=\frac{a^{\mathrm{H}}(\omega,\theta,\phi)\Sigma^{-1}\hat{R}\Sigma^{-1}a(\omega,\theta,\phi)}{\mathrm{tr}(\Sigma^{-1}\hat{R})\cdot\eta(\theta,\phi)}, \qquad (8)$$

$$L_N=N(D-1)-1. \qquad (9)$$

We can see the extent of estimation accuracy visually by checking the posterior distribution $p(\theta,\phi\mid\hat{R})$. We can easily calculate the estimated values of θ and ϕ denoted as $\hat{\theta}$ and $\hat{\phi}$ respectively), which can be expressed as:

$$\hat{\theta}\approx\sum_{m=1}^{M}\theta_m P(\theta_m,\phi_m\mid\hat{R}), \qquad (10)$$

$$\hat{\phi}\approx\sum_{m=1}^{M}\phi_m P(\theta_m,\phi_m\mid\hat{R}), \qquad (11)$$

$$P(\theta_m,\phi_m\mid\hat{R}):=\frac{p(\theta_m,\phi_m\mid\hat{R})}{\sum_{m'=1}^{M}P(\theta_{m'},\phi_{m'}\mid\hat{R})}, \qquad (12)$$

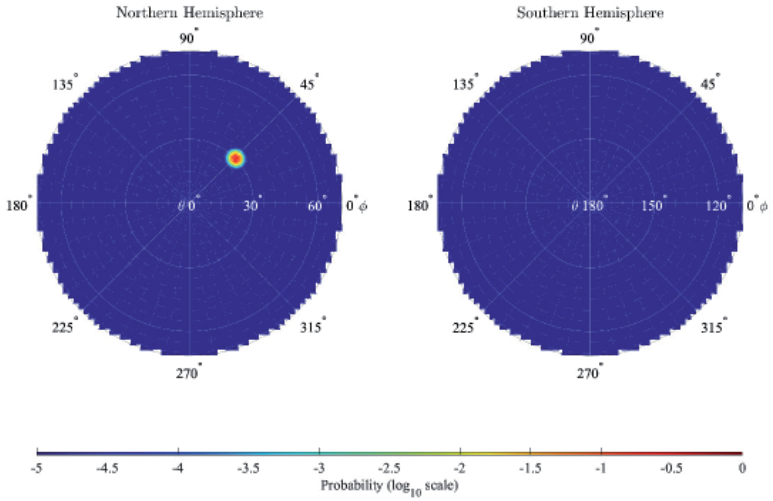

Figure 1: Estimation results of the proposed method with $D=6$ (the electromagnetic field components) and $N=16$

where (θ_m,ϕ_m) (m = 1,…, M) is the discretized direction of arrival, and M is the number of the grids. We can also easily calculate the variances of θ and ϕ denoted as σ_θ^2 and σ_ϕ^2 respectively) by:

$$\sigma_\theta^2 \approx \sum_{m=1}^{M}\left(\theta_m-\hat{\theta}\right)^2 P\left(\theta_m,\phi_m \mid \hat{R}\right), \tag{13}$$

$$\sigma_\phi^2 \approx \sum_{m=1}^{M}\left(\phi_m-\hat{\phi}\right)^2 P\left(\theta_m,\phi_m \mid \hat{R}\right). \tag{14}$$

3. Evaluation through Simulations

We conducted relevant simulations using the spectral matrices estimated from the pseudo-observed signals to simulate different numbers of sensors D and averaging numbers N of the spectral matrix.

3.1 Evaluation Specifications

The pseudo-observed signal was generated as a narrow-band signal with thermal noise. Considering the case where the electromagnetic field sensor is placed in the positive direction of the x-, y- and z- axes, with the z-axis being parallel to the external magnetic field.

The pseudo-observed signal $x(t,\omega)\in\mathbb{C}^D$ can be expressed as:

$$x(t,\omega)=s(t)\,a(\omega,\theta_s,\phi_s)+n(t). \tag{15}$$

Here, $s(t)$ is the complex amplitude in the direction of arrival (θ_s,ϕ_s) following a zero-mean complex Gaussian

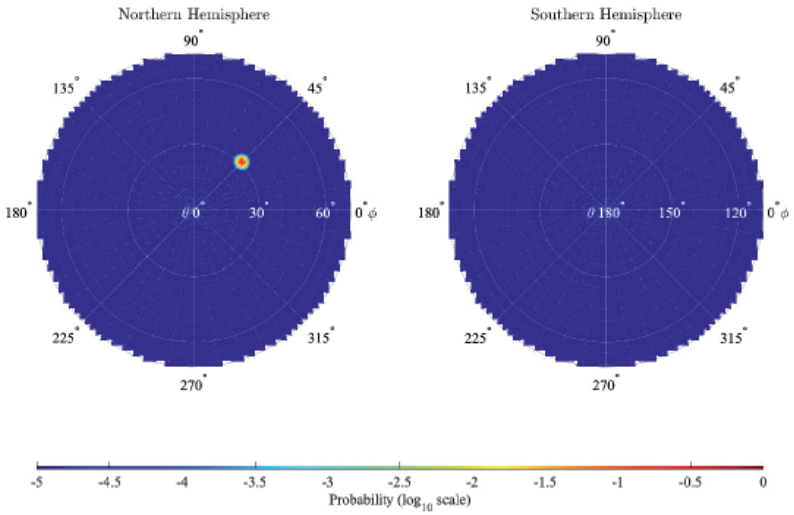

Figure 2: Estimation results of the proposed method with $D=6$ the electromagnetic field components) and $N=32$

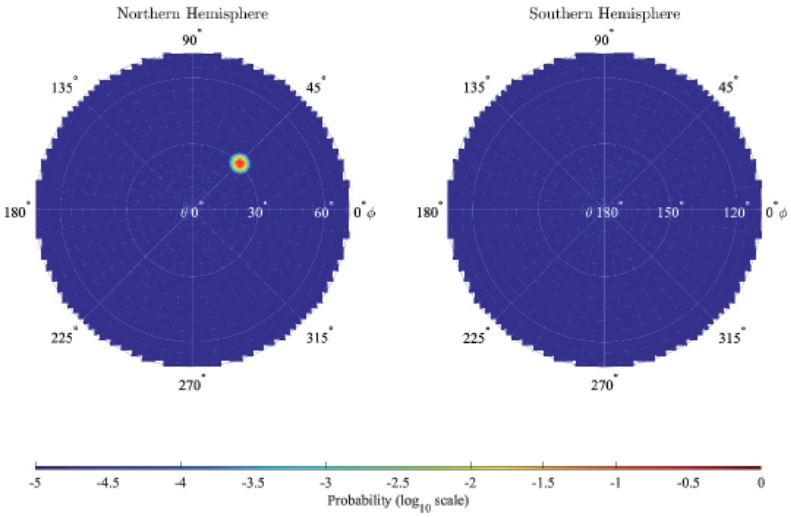

Figure 3: Estimation results of the proposed method with $D=5$ (without the E_z component)

process with a variance of σ_s^2 and $n(t) \in \mathbb{C}^D$ is the thermal noise applied to each channel of the electromagnetic field sensor, following a zero-mean complex Gaussian process with a covariance matrix of εI_D where I_D is the identity matrix of an order of D. We set the direction of arrival θ_s and ϕ_s as 30° and 45° respectively, and set the signal-to-noise ratio (SNR) parameter σ_s^2 / ε as 20 dB. We also assumed that $s(t)$ and $n(t)$ are uncorrelated. The estimated value of the spectral matrix $\hat{R}$ was calculated from Equation (3) using the generated pseudo-observed signal $x(\nu\Delta T, \omega)(\nu = 1, ..., N)$ obtained from Equation (15). To obtain the steering vector $a(\omega, \theta, \phi)$, we set the propagation mode to the R-X mode, the frequency $\omega / 2\pi$ to 1.000 kHz, the plasma frequency to 6.655 kHz, and the cyclotron frequency of electrons to 3.540 kHz. In the simulation setup, the refractive index was 4.8 and the SNR of the electric field and the magnetic field were 7.6 and 19.7 dB, respectively. Then, we used Equation (5) to visualize the extent of estimation accuracy and calculated Equations (10) to (14) by using the calculated $\hat{R}$. We discretized the direction of arrival (θ_m, ϕ_m) (m = 1,..,M) using Appendix A in Tanaka *et. al* [6] with the number of the grids $M = 5,704$.

We conducted simulations with different numbers of sensors including $D=6$ (the electromagnetic field components) and $D=5$ (without E_z or $Z_0 H_z$) where H_z is multiplied by the characteristic impedance of vacuum, denoted as Z_0 in order to convert the dimension of the magnetic field to match that of the electric field. Even when $D=5$, the absolute k-vector direction can still be estimated by Faraday's law, but note that the SNR of $Z_0 H_z$ was higher than that of E_z in our simulation setup. We set N as 16 and 32 (two patterns) to check if the extent of estimation accuracy would increase by increasing N.

3.2 Simulation Results

The estimation results of the proposed method can be found in Figures 1 to 4. More specifically, the estimation results of the electromagnetic field components with the averaging number $N=16$ and 32 are shown in Figures 1 and 2, respectively. The electromagnetic field components without E_z and $Z_0 H_z$ are shown in Figures 3 and 4, respectively. The radius of the estimation results represents the zenith angle θ and the circumference angle of the estimation results represents the azimuth angle ϕ. The posterior probability of the proposed method $P(\theta_m, \phi_m \mid \hat{R})$ (m = 1,…, M) is represented by different colors from blue to red. The parameters from Equations (10) to (14) in Figures 1 to 4 are summarized in Table 1.

As shown in Figure 1, it can be found that the peak of $P(\theta_m, \phi_m \mid \hat{R})$ was around the true value $(\theta_s, \phi_s) = (30^\circ, 45^\circ)$,

Table 1: Parameters calculated from Equations (10) to (14)

Specification	$\hat{\theta} \pm \sigma_\theta [^\circ]$	$\hat{\phi} \pm \sigma_\phi [^\circ]$
Case in Figure 1	29.52 ± 1.05	44.01 ± 2.18
Case in Figure 2	30.26 ± 0.62	45.05 ± 1.17
Case in Figure 3	29.68 ± 1.01	44.36 ± 2.08
Case in Figure 4	26.37 ± 2.75	45.75 ± 7.91
True value	30	45

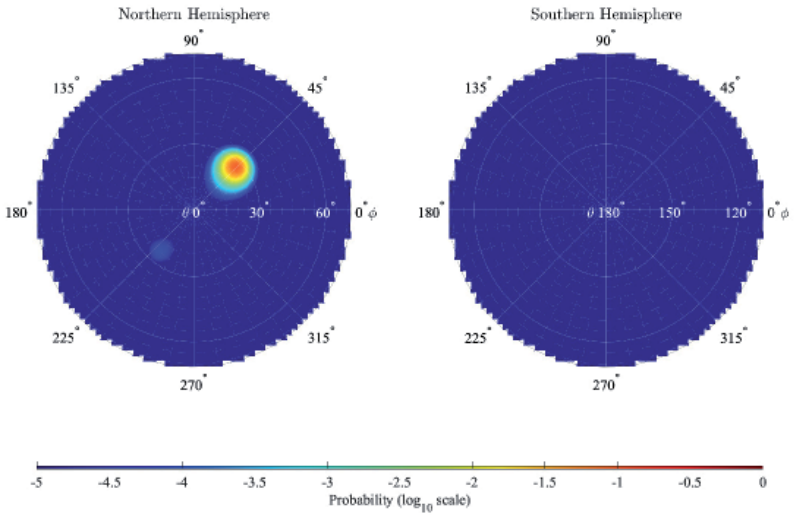

Figure 4: Estimation results of the proposed method with $D=5$ (without the Z_0H_z component) and $N=16$

indicating that the proposed method can correctly visualize the extent of estimation accuracy.

In Figure 2, it was shown that the peak of $P(\theta_m,\phi_m|\hat{R})$ was sharper than that in Figure 1. From Table 1, it was also found that the estimated value $\hat{\theta}$ and $\hat{\phi}$ in Figure 2 improved by 0.2 and 1.0 deg, respectively. Moreover, the standard deviations σ_θ and σ_ϕ in Figure 2 decreased by 0.4 and 1.0 deg, respectively. These findings indicated that when the averaging number *N* increased, the extent of estimation accuracy also increased accordingly.

As shown in Figure 3, it was found that the estimation results were almost the same as those in Figure 1. Comparatively, the peak of $P(\theta_m,\phi_m|\hat{R})$ in Figure 4 demonstrated a broader peak, and the errors of the estimation values and the variances of θ and ϕ were larger, as shown in Table 1. This indicated that the proposed method can demonstrate the importance of Z_0H_z in the simulation setup, as it showed a higher SNR than E_z both visually, and numerically.

4. Summary and Future Work

In this study, we proposed the Bayesian *k*-vector estimation method in magnetized cold plasma based on the WDF method. Our proposed method was found robust under different sensor noise levels since the NIK can estimate *k*-vector direction even when the number of sensors is very few, due to the adoption of the Bayesian inference. We verified that the proposed method can visualize and calculate the extent of estimation accuracy and identify which sensor is important for estimation.

Our future work is to evaluate the proposed method when the noise levels are different among the sensors, or the number of the sensors is less than 5.

5. Acknowledgments

This research was partially supported by the Grant-in-Aid for Scientific Research from the Japan Society for the Promotion of Science (Grant Number: 21H01146). This research was also financially supported by the Support for Pioneering Research Initiated by the Next Generation program by the Japan Science and Technology Agency (Grant Number: JPMJSP2135). The authors would like to thank Enago (www.enago.jp) for the English language review.

6. References

1. C. A. Kletzing, W. S. Kurth, M. Acuna, R. J. MacDowall, R. B. Torbert, T. Averkamp, D. Bodet, S. R. Bounds, M. Chutter, J. Connerney, D. Crawford, J. S. Dolan, R. Dvorsky, G. B. Hospodarsky, J. Howard, V. Jordanova, R. A. Johnson, D. L. Kirchner, B. Mokrzycki, G. Needell, J. Odom, D. Mark, R. Pfaff, J. R. Phillips, C. W. Piker, S. L. Remington, D. Rowland, O. Santolik, R. Schnurr, D. Sheppard, C. W. Smith, R. M. Thorne and J. Tyler, ``The Electric and Magnetic Field Instrument Suite and Integrated Science (EMFISIS) on RBSP,'' *Space Science Reviews*, **179**, 1, November 2013, pp. 127-181.

2. Y. Kasahara, Y. Kasaba, H. Kojima, S. Yagitani, K. Ishisaka, A. Kumamoto, F. Tsuchiya, M. Ozaki, S. Matsuda, T. Imachi, Y. Miyoshi, M. Hikishima, Y. Katoh, M. Ota, M. Shoji, A. Matsuoka and I. Shinohara, ``The Plasma Wave Experiment (PWE) on Board the Arase (ERG) Satellite,'' *Earth, Planets and Space*, **70**, 1, November 2013, pp. 86.

3. O. V. Agapitov, D. Mourenas, A. V. Artemyev, F. S. Mozer, G. Hospodarsky, J. Bonnell and V. Krasnoselskikh, ``Synthetic Empirical Chorus Wave Model from Combined Van Allen Probes and Cluster Statistics,'' *Journal of Geophysical Research: Space Physics*, **123**, 1, January 2018, pp. 297-314.

4. L. R. O. Storey and F. Lefeuvre, ``The Analysis of 6-Component Measurements of a Random Electromagnetic Wave Field in a Magnetoplasma - I. The Direct Problem,'' *Geophysical Journal International*, **56**, 2, February 1979, pp. 255-269.

5. L. R. O. Storey and F. Lefeuvre, ``The Analysis of 6-Component Measurements of a Random Electromagnetic Wave Field in a Magnetoplasma - II. The Integration Kernels,'' *Geophysical Journal International*, **62**, 1, July 1980, pp. 173-194.

6. Y. Tanaka, M. Ota and Y. Kasahara, ``Noise Integration Kernel Design for the Wave Distribution Function Method: Robust Direction Finding With Different Sensor Noise Levels,'' *Radio Science*, **56**, 9, August 2021, pp. e2021RS007291.

7. H. L. Van Trees, *Optimum Array Processing*, New York, United States, Wiley-Interscience, 2002.

8. P. Shaman, ``The Inverted Complex Wishart Distribution and Its Application to Spectral Estimation,'' *Journal of Multivariate Analysis*, **10**, 1, March 1980, pp. 51-59.

9. Y. Tanaka, M. Ota and Y. Kasahara, ``Identification Approach of Arriving Wave Model Based on Likelihood Ratio Test With Different Sensor Noise Levels,'' *Radio Science*, **57**, 8, July 2022, pp. e2022RS007427.